

# Dipolar interactions in magnetic nanowires aggregates.

Thomas Maurer,

*Laboratoire de Nanotechnologie et d'Instrumentation Optique, ICD CNRS UMR STMR 6279,  
Université de Troyes, BP 2060, 10010 Troyes cedex, France\**

Fatih Zighem, Weiqing Fang, Frédéric Ott, Grégory Chaboussant

*Laboratoire Léon Brillouin, IRAMIS, CEA-CNRS UMR 12, CE-Saclay, 91191 Gif sur Yvette, France*

Yaghoub Soumare, Kahina Ait Atmane and Jean-Yves Piquemal

*ITODYS Université Paris 7 - Denis Diderot, UMR CNRS 7086,  
2, place Jussieu F-75251 Cedex 05 Paris, France*

Guillaume Viau

*Université de Toulouse, LPCNO, INSA, UMR CNRS 5215,  
135, avenue de Rangueil, F-31077 Toulouse Cedex 4.*

We investigate the role of dipolar interactions on the magnetic properties of nanowires aggregates. Micromagnetic simulations show that dipolar interactions between wires are not detrimental to the high coercivity properties of magnetic nanowires composites even in very dense aggregates. This is confirmed by experimental magnetization measurements and Henkel plots which show that the dipolar interactions are small. Indeed, we show that misalignment of the nanowires in aggregates leads to a coercivity reduction of only 30%. Direct dipolar interactions between nanowires, even as close as 2 nm, have small effects (maximum coercivity reduction of  $\sim 15\%$ ) and are very sensitive to the detailed geometrical arrangement of wires. These results strengthen the potential of magnetic composite materials based on elongated single domain particles for the fabrication of permanent magnetic materials.

PACS numbers: 75.50.Ww, 75.50.-y, 75.75.-c, 81.07.Gf

Keywords: magnetic nanowires, aggregates, micromagnetic simulations, magnetization curves, dipolar interactions

## I. INTRODUCTION

Taking advantage of the shape anisotropy for the fabrication of high coercivity materials has been considered in the past. We can mention the development of elongated single domain (ESD) particles [1–3] or the AlNiCo materials [4] in which elongated magnetic structures are formed by a proper metallurgical process. These materials are however limited in their performances to coercive fields of the order of a few mT. During the last decade it has been shown that elongated magnetic nano-objects with well defined shapes could be synthesized [5–9]. We have considered the use of magnetic nanorods for the fabrication of high magnetic energy polymer composite materials. We have shown that rather high coercive fields, up to 600 kA/m ( $= 0.75$  T) could be obtained [10]. However, the nanowires are not optimally dispersed in the matrix material and tend to form aggregates (Figure 1). The scope of this communication is to address the role of the dipolar interactions in nanowire aggregates on the coercive field in our composite materials.

The role of dipolar interactions in assemblies of magnetic nanoparticles has already been addressed in several situations. In some geometries, such as planar arrays of

magnetic nanowires fabricated in porous alumina membranes, the dipolar fields play a very important role. It has been experimentally demonstrated that the demagnetizing field  $H_d$  is simply proportionnal to the packing density  $P$ :  $H_d = -P.M_s$  [11, 12]. Since  $P$  can reach values up to 30%, the demagnetizing fields are very large and significantly reduce the coercivity and more generally the anisotropy properties of the arrays [12, 13].

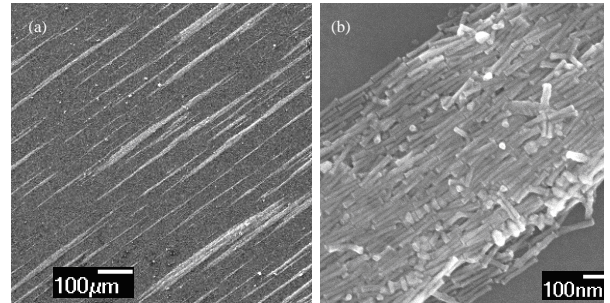


Figure 1. Scanning Electron Microscope images of *Co* nanowires deposited under a magnetic field on a *Si* substrate. (a) At the microscopic scale, the objects form microstructures with cigar shapes. (b) Inside these microscopic structures, the *Co* nanowires are rather well aligned with an angular dispersion of the order of  $\sigma = 7^\circ$ .

\* thomas.maurer@utt.fr

The effects of dipolar fields have also been considered

for granular hard magnetic materials [14]. In this case, Henkel plots [15] -obtained from isothermal remanent magnetization and dc demagnetization experiments- allow to put into evidence interactions between magnetic grains [16]. In the above situations macroscopic demagnetizing field effects must be taken into account. In our composite materials, the situation is qualitatively different since elongated cigar shape aggregates are formed. Thus macroscopic demagnetizing field effects, within a cigar, are expected to be negligible. In this communication we focus on local dipolar field effects between individual wires and we use micromagnetic simulations to quantify the role of the magnetic interactions between nanowires on the coercive field.

## II. MAGNETIC NANOWIRES AND AGGREGATES

We consider the experimental case of  $Co$  and  $Co_{80}Ni_{20}$  nanowires synthesized via the polyol process [5–8]. These nanowires exhibit diameters in the range 7 – 15 nm and lengths in the range 100–250 nm. In the previous studies, these nanowires, either randomly oriented or well-aligned in solvents, have been magnetically characterized. The experimental hysteresis cycles have been discussed within the Stoner-Wohlfarth model [10]. The reversal mechanism is usually not a coherent one and it is initiated at the wires tips. Micromagnetic simulations put into evidence the role of the detailed shape of these objects in the magnetization reversal [17]. The chemical synthesis of magnetic wires has been optimized to achieve a cylindrical shape so as to optimize the shape anisotropy [7].

When the nanowires are dispersed in solvents and dried under a magnetic field, they tend to form microscopic aggregates (Fig. 1) so that there can be direct magnetic dipolar interactions between the objects. The nanowires are covered with an oxide shell which is typically 1 – 2 nm thick [18] so that the minimal distance between the ferromagnetic cores is of the order of 2 – 4 nm.

Figure 2 represents the dipolar stray field at the tip of a nanowire ( $L = 100$  nm,  $r = 5$  nm,  $M_s = 1$  T) calculated using FEMM [19]. It illustrates that the dipolar field is very localized around the tip (in a volume with a typical size given by the radius of the nanowire). The stray fields are of the order of 0.1 T at a distance of 4-7 nm from the nanowire tip (see Fig. 2b). Thus, since the nanowires are separated by distances which can be as small as 2 – 4 nm, the dipolar field radiated by one wire on its neighbors can still be of the order of a fraction of one Tesla.

In the present paper, we address the question whether global or local stray fields may significantly affect the magnetic properties of nanowire aggregates. Several effects may play a role in modifying the overall coercivity of nanowires assemblies. They can be classified in the following way:

(i) The wires may be disoriented with respect to each other. This leads to a significant loss in the macroscopic

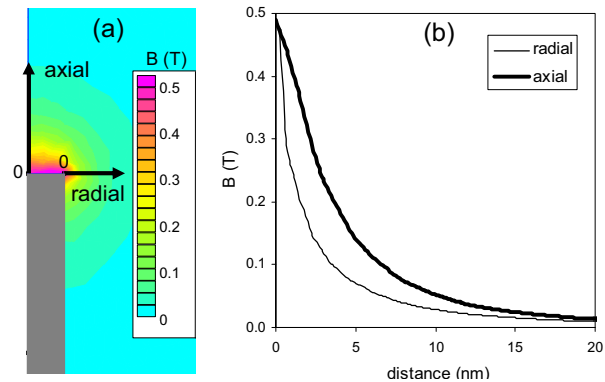


Figure 2. Dipolar field outside the tip of a ( $L = 100$  nm,  $r = 5$  nm,  $M_s = 1$  T) magnetic nanowire (gray area) calculated using FEMM [19]. (a) Axial mapping of the induction outside the wire. (b) Magnitude of the induction along the wire axis and the radial axis. The dipolar stray fields drop quickly but are still of the order of 0.1 T at a distance of 4 – 7 nm of the wire edges.

coercivity.

(ii) The fact that the wires are assembled in cigar shaped structures has in principle the effect of decreasing the macroscopic demagnetizing field effects and increasing the overall coercivity.

(iii) The local stray fields created by a wire tip may create a local nucleation point and promote the reversal of a neighboring wire.

(iv) The presence of “defective wires” with low coercivity because of a poorly defined shape, a strong misorientation, or a structural defect may play the role of a nanoscopic nucleation point inside the cigar microstructure.

In the following, we quantify these different effects in order to estimate the requirements for obtaining composite materials with optimum coercivity properties.

## III. MODELLING

The model objects which are considered are cylindrical objects of length  $L = 100$  nm and radius  $r = 5$  nm. The magnetic parameters used correspond to *hcp* cobalt epitaxial thin films [20], saturation magnetization  $M_S = 1400$  kA.m<sup>-1</sup>, exchange constant  $A = 1.2 \times 10^{-11}$  J/m. The micromagnetic calculations have been performed using the *Nmag* package [21]. The objects were meshed using *Netgen* [22] with meshes consisting of about 1000 points so that the distance between two nodes is of the order of the exchange length  $\ell_{ex} = \sqrt{2A/\mu_0 M_S^2} \approx 3.2$  nm. Increasing the finesse of the meshes did not change the results. Magnetocrystalline anisotropy was not included in the calculation on purpose so as to avoid masking the dipolar effects by extra anisotropy effects. Adding an extra magnetic anisotropy to the wires would not change the conclusions.

### A. Orientation effects

For perfectly aligned infinite ellipsoids, the expected coercive field (obtained from the shape anisotropy) is  $M_S/2$  that is  $700 \text{ kA/m}$  ( $\equiv 0.88T$ ) in the considered experimental situation. However, in the case of nanowires of finite length instead of infinite ellipsoids, a significant drop in the shape anisotropy is expected ( $\sim 25\%$ )[17]. On top of that, the misorientation of the nanowires induces a loss in the effective coercivity. We assume a Gaussian distribution. Let  $\sigma$  be the width of the distribution of the wires orientations with respect to the applied field.  $H_c$  drops from  $0.38 M_S$  for a very narrow orientation distribution ( $\sigma = 1^\circ$ ) down to  $0.21 M_S$  for a random orientation distribution (see Fig. 3). In the observed situation of Figure 1, the angular distribution of wires has a width of about  $\sigma = 7^\circ$  leading to a moderate loss of coercivity ( $\sim 15\%$ ) compared to  $\sigma = 1^\circ$ . Thus extremely well aligned nanowires do not significantly boost the performances of the material.

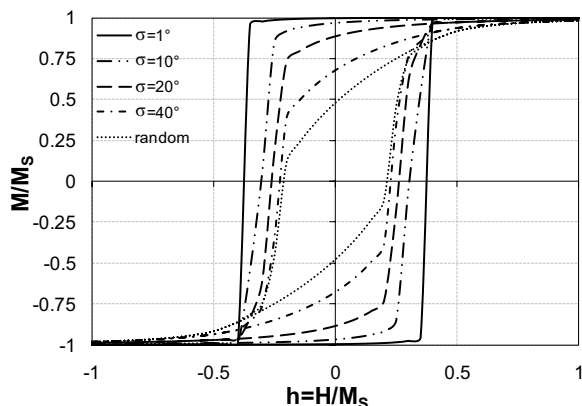


Figure 3. Hysteresis cycles for different wires orientation distributions:  $\sigma = 1^\circ, 10^\circ, 20^\circ, 40^\circ, \infty$ (random). In the experimental situation of Figure 1,  $\sigma$  has been estimated at  $7^\circ$ .

### B. Demagnetizing field effects

The assembly of the wires into cigar shape structures potentially modifies the overall demagnetization field distribution. To account for this effect we have compared the following 3 situations: (A1) an isolated wire, (A2) a chain of 2 wires separated by  $l = 2 \text{ nm}$ , (A3) a chain of 3 wires (Fig. 4). The separation of  $2 \text{ nm}$  which is a minimum value, corresponds to the experimental situation because the wires are surrounded by a shell of non magnetic material which prevents a direct contact between the wires. The reference value of the coercive field for an isolated wire is  $H_C \approx 375 \text{ kA/m}$ . The micromagnetic simulations show that no measurable change in the coercive field is observed when the wires are arranged in chains. This could be expected since the wires already

have a large aspect ratio so that we are very close to the case of infinite cylinders. The demagnetizing coefficient  $N$  of an ellipsoid of aspect ratio 10 is equal to  $0.02$  which is very close to the value  $N = 0$  for an infinite cylinder. Increasing further the overall aspect ratio does not induce measurable effects. When the magnetic field is applied at an angle (ranging from  $0^\circ$  to  $20^\circ$ ) with respect to the chains, no measurable change in the coercivity are observed between the A1, A2 and A3 configurations.

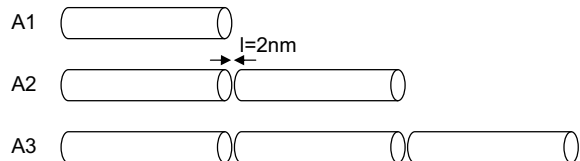


Figure 4. Wires configurations used in the calculations. (A1) A single wire which is the reference situation. (A2) A chain of 2 wires separated by  $2 \text{ nm}$ . (A3) A chain of 3 wires.

### C. Effect of local stray fields

We have considered several situations in which the stray field of a wire tip may alter the reversal of a neighboring wire. We have considered 2 main situations: (i) the case where the stray field acts at a wire tip (B1 - B2), (ii) the case where the stray field acts on a neighboring wire edge (B3). The different configurations are illustrated on Figure 5. We first focused on the situation of aligned nanowires before considering misalignment which is recurrent in aggregates. The angle between the two nanowires long axes is noted  $\alpha$ .

Figures 6(a), (b) and (c) respectively display the hysteresis cycles of the B1, B2 and B3 configurations for different values of the  $\alpha$  angle. For the B1 and B2 configurations with  $\alpha = 0$ , the hysteresis cycles are identical to the one of a single nanowire and  $H_C \approx 375 \text{ kA/m}$  (Fig. 6a and b). It implies that for these configurations -close to A2- there is no measurable effect of the local stray field on the wire tips. Both wires switch at the same time. The situation differs for the B3 configuration where the stray field acts on a neighboring wire edge. In this case, the coercivity is lowered to  $H_C \approx 325 \text{ kA/m}$ , that is a loss of  $13\%$ , while the cycle remains almost perfectly square (Fig. 6c). The magnetization reversal of both nanowires is simultaneous.

We now investigate the effects of misorientations ( $\alpha \neq 0$ ) for the configurations B1, B2 and B3 in order to reproduce the situation of aggregates. In the B1 configuration, the coercive field is reduced from  $H_C \approx 375 \text{ kA/m}$  for  $\alpha = 0^\circ$  down to  $H_C \approx 255 \text{ kA/m}$  for  $\alpha = 40^\circ$ . The magnetization reversal of both nanowires remains simultaneous demonstrating that there is a strong interaction between the wires. However in the limiting case where  $\alpha = 90^\circ$  (*i.e.* the nanowires are perpendicular to each other), the

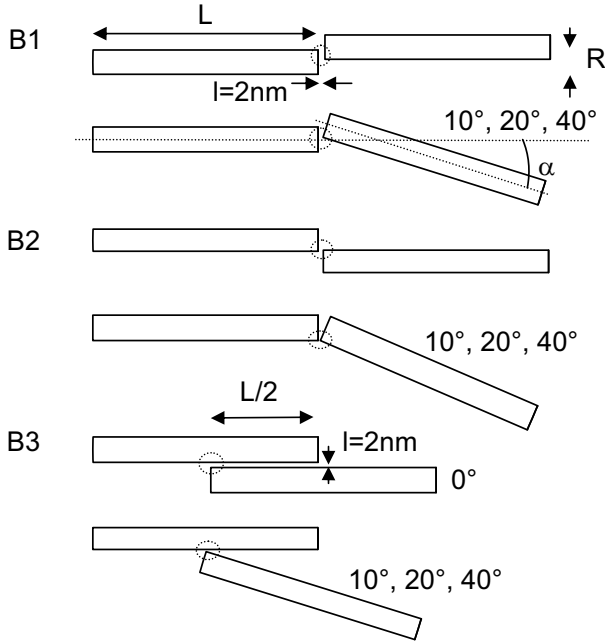


Figure 5. Wires configurations used in the calculations. (B1) Two wires touching at their tips but shifted by  $R$ . The relative orientation of the wires can vary from  $\alpha = 0^\circ$  to  $40^\circ$ . (B2) Two wires touching at their tips but shifted by  $2R$ . (B3) A wire creating a stray field around the center of another wire.

coercive field is somewhat recovered to  $H_C \approx 330$  kA/m but the two wires reversals are disconnected. The magnetization of the wire at  $90^\circ$  simply follows a linear dependence with respect to the applied field.

The situation slightly differs in the  $B2$  configurations since the magnetization reversal of both nanowires is no more simultaneous for  $\alpha = 20^\circ$  and  $40^\circ$  showing that the interactions between wire tips is very sensitive to geometrical details. Furthermore, in the limiting case  $\alpha = 90^\circ$ , the coercivity almost recovers the value of the isolated nanowire case, suggesting that there are no more measurable interactions between the wires.

The situation is qualitatively different in the  $B3$  configurations. Figure 6(c) shows that for  $\alpha = 10^\circ, 20^\circ$  or  $40^\circ$ , the magnetization reversal of both nanowires is no more simultaneous and the coercivity of the aligned wires recovers a value of  $H_C \approx 375$  kA/m corresponding to the case of an isolated wire ( $A1$ ). Surprisingly, it shows that neighboring wires in the configurations  $B3$  have measurable effects on the coercive field only when they are parallel to their neighbor and that as soon as there is a small misalignment, there are no more interactions.

Finally, on the one hand, for perfectly aligned wires ( $\alpha = 0^\circ$ ), stray fields leads to a moderate loss of coercivity (13%) only in the  $B3$  configuration. On the other hand, misalignment of the nanowires ( $\alpha \neq 0^\circ$ ), induces a significant loss of coercivity in the  $B1$  and  $B2$  configurations while stray fields effects become negligible in the

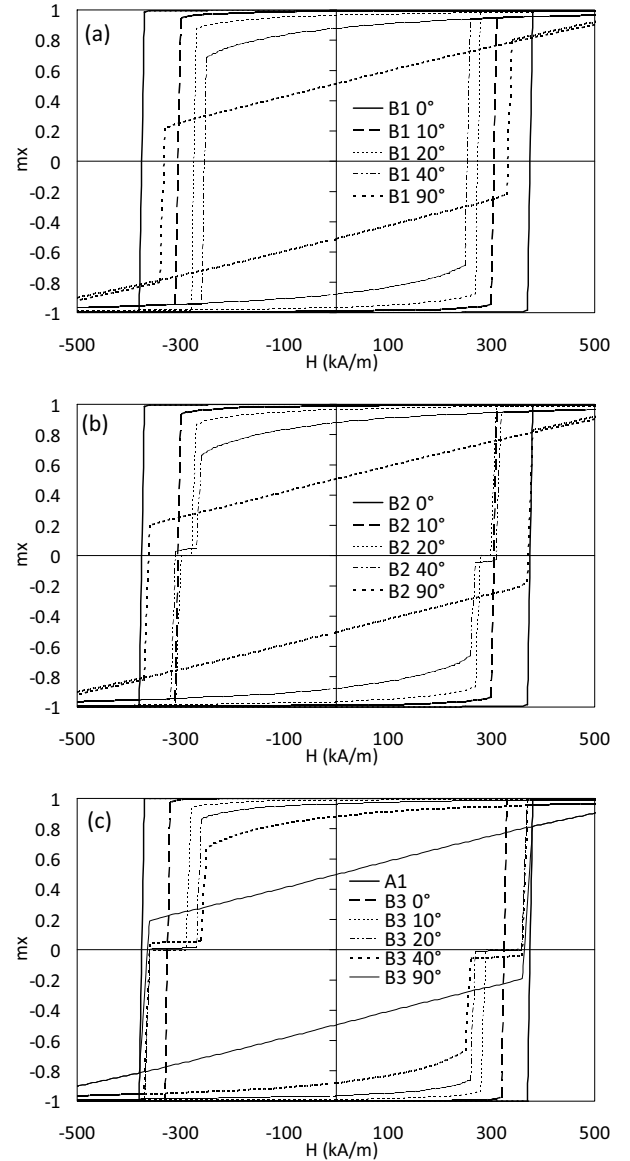


Figure 6. Hysteresis cycles of the (a)  $B1$  configuration for  $\alpha = 0^\circ, 10^\circ, 20^\circ, 40^\circ$  and  $90^\circ$ , (b) Hysteresis cycles of the  $B2$  configuration for  $\alpha = 0^\circ, 10^\circ, 20^\circ, 40^\circ$  and  $90^\circ$ , (c) Hysteresis cycles of the  $B3$  configuration for  $\alpha = 0^\circ, 10^\circ, 20^\circ, 40^\circ$  and  $90^\circ$ .

$B3$  configurations. The dipolar interactions on the coercivity are very sensitive to the geometrical arrangement of wires.

#### D. Effect of nanoscopic nucleation or pinning points

We now consider the case of nucleation or pinning points created inside a cigar shaped micro-structure by wires which have respectively either a lower coercivity

or a higher coercivity. In the case of a wire with a geometrical defect, corked or with 3 endings for example, its coercivity will be decreased. On the other hand, one may imagine that some wires contain structural defects which pin their magnetization. For the micro-magnetic modelling, we have thus pinned the magnetization  $M_0$  of one of the wires of the structure in a direction along the nanowire long axis (Fig. 7 top). Starting from a negative saturation field  $-H_{sat}$ , when arriving at remanence, none of the wires has flipped except for the pinned one. This pinned wire can thus be considered as a nucleation point which will promote the reversal of neighboring wires when the field is further increased. A loss of coercivity is expected. On the other hand, starting from a positive saturation field  $+H_{sat}$ , when arriving at remanence, the magnetization of all the wires are still parallel. When the field is further decreased, the pinned wire will not flip and will thus act as a pinning point. A slight increase in coercivity is expected. Thus, on the calculated hysteresis cycle, the effect of pinning can be observed on the left side while on the right side, the effect of nucleation is observed.

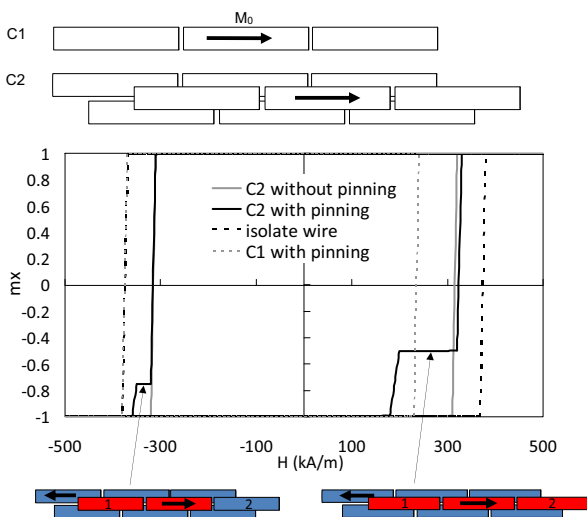


Figure 7. Various configurations of aggregated wires in which the magnetization of one of the wire is pinned. (C1) Chain of 3 wires. (C2) Staggered rows of wires.

We performed micromagnetic simulations on various configurations of aggregated wires. Let us discuss the two situations illustrated in the geometries of Fig. 7 (top). In the first case, we look at the behavior of a row of 3 wires in which the middle one has its magnetization pinned. The hysteresis cycles of Fig. 7 show the evolution of the magnetization of the free wires. That is we plot the average magnetization (normalized to one) of all the wires except the pinned one. The reference situation of an isolated wire is represented as the black dashed line. When the field is swept to negative values, the coercive field of the wires chain is unchanged with respect to the

isolated wire: the pinned wire has no effect. On the other hand, when sweeping the field to positive values, the pinned wire acts as a strong nucleation point and induces a 40% drop of the coercive field with respect to an isolated wire. The configuration C2 consists of 9 wires among which one is pinned. The reference situation (9 free wires) is plotted on Fig. 7 as the solid grey line. The coercivity is 317 kA/m. In the C2 configuration, when the field is swept to negative values, the coercive field of the wires chain is unchanged. There is only a small step which appears in the hysteresis cycle which corresponds to a stiffer reversal for the Nr. 1 wire (see small sketch of Figure 7). We suggest that the different behaviour of wires 1 and 2 is due to demagnetizing field effects. When sweeping the field to positive values, the pinned wire acts as a strong nucleation point and promotes a first reversal of wires 1 and 2 at a field 40% lower than the coercive field. The other wires behavior is barely modified. The coercivity is slightly increased which can be accounted for by dipolar interactions with the flipped row. Thus, in conclusion, a pinned wire only affects the behavior of its neighbor along a chain but not its side neighbors.

#### IV. EXPERIMENTAL RESULTS

In order to probe the interactions in granular magnetic materials, Henkel [15] proposed to compare the Isothermal Remanent Magnetization (IRM) and Direct Current Demagnetization (DCD) curves. The difference  $\delta m(H) = (2.IRM(H) - DCD(H))/IRM(\infty) - 1$  being either zero in the case of non interacting particles [23], positive for interactions promoting the magnetized state and negative for interactions assisting magnetization reversal. Note that we are measuring the DCD with an initial negative saturation field which is opposite to the usual convention, hence the change of sign in the previous formula for the DCD contribution. We think that this way of measuring the DCD is more natural though.

We performed IRM and DCD measurements on aligned Co nanowires deposited on a Si substrate (see Fig. 1). The measurements were performed both parallel and perpendicular to the easy axis of the nanowires aggregates (Fig. 8). One can notice that  $\delta m(H)$  is mostly zero except in 2 small regions during the reversal process. The  $\delta m(H)$  value is small (max  $\sim -14\%$ ) and negative suggesting that only dipolar interactions assisting reversal take place. This is in agreement with the above calculations by showing that (i) forming aggregates does not stabilize the magnetic structures and that only extra nucleations can be induced by dipolar effects and (ii) that these effects remain rather small even in very compact structures with densities close to 1. No qualitative difference is observed in the measurements along and perpendicular to the easy axis. The facts that two small peaks are observed in  $\delta m(H)$  during the reversal process suggests that different mechanisms are taking place at the beginning and at the end of the aggregate reversal. This

needs to be investigated further.

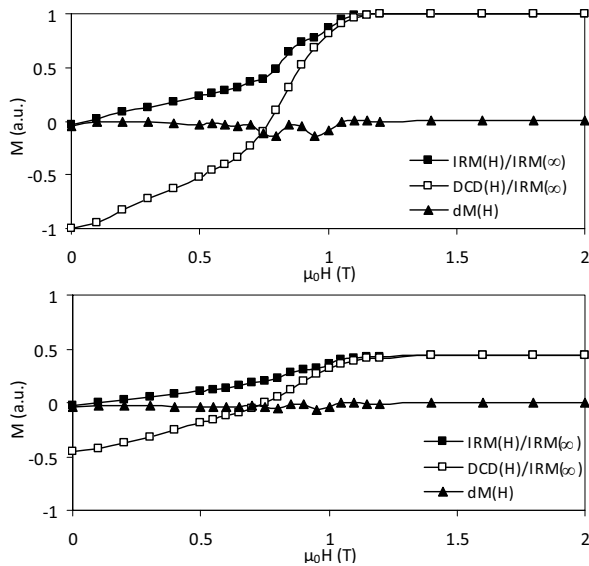


Figure 8. IRM, DCD and Henkel plots measured on aligned Co wires in a polymer matrix. The magnetic field was applied either parallel (top) or perpendicular (bottom) to the aggregates axis.

## V. CONCLUSION AND PERSPECTIVES

We have investigated the role of magnetic dipolar interactions between nanowires in aggregates via micromagnetic simulations. In the case of aggregates composed of perfectly aligned nanowires, these simulations show that no major change should be observed in the shape of the hysteresis cycles or in the values of the coercivity and the remanence. In the worst situation a drop of 20% in the coercive field might be observed. We underline that local dipolar interactions effects on the coercivity are very sensitive to the detailed geometrical arrangement of wires. As for the effect of nanowire misalignment inside aggregates, we show that even very poor alignment leads only to a 30% reduction in the coercive field. Using Henkel plots we have experimentally confirmed that dipolar effects are indeed small in these aggregates of nanowires or that at least they do not significantly modify the magnetic behavior. This validates the way of interpreting the experimental magnetic hysteresis cycles in [10].

It is striking that in dense aggregates of magnetic nanowires, dipolar interactions play a very limited role. We conclude that in dense materials based on magnetic nanowires, the interactions between wires are negligible and that the optimization of the properties goes through the optimization of the properties of individual wires.

## ACKNOWLEDGMENTS

The authors gratefully acknowledge the Agence Nationale de la Recherche for their financial support (project P-Nano MAGAFIL). We thank J.B. Moussy (CEA-IRAMIS) for his help in the magnetometry measurements.

- 
- [1] L.I. Mendelsohn, F.E. Luborsky, T.O. Paine, *J. Appl. Phys.* **26**, 1274-1280 (1955).
  - [2] R.B. Falk, *J. Appl. Phys.* **37**, 1108-1112 (1966).
  - [3] D.J. Craik, R. Lane, *J. Appl. Phys.*, **18**, 1269-1274 (1967).
  - [4] R. O'Handley, *Modern Magnetic Materials, Principles and Applications*, p.480 (Wiley Intersciences, New York, 2000).
  - [5] D. Ung, G. Viau, C. Ricolleau, F. Warmont, P. Gredin, and F. Fiévet, *Adv. Mater.*, **17**, 338 (2005).
  - [6] D. Ung, Y. Soumare, N. Chakroune, G. Viau, M.-J. Vaulay, V. Richard, F. Fiévet, *Chem. Mater.*, **19**, 2084 (2007).
  - [7] Y. Soumare, J.-Y. Piquemal, T. Maurer, F. Ott, G. Chaboussant, A. Falqui and G. Viau, *J. Mater. Chem.* **18**, 5696-5702 (2008).
  - [8] Y. Soumare, C. Garcia, T. Maurer, G. Chaboussant, F. Ott, F. Fiévet, J.-Y. Piquemal and G. Viau, *Adv. Func. Mater.* **19**, 1-7 (2009).
  - [9] K. Soulantica, F. Wetz, J. Maynadié, A. Falqui, R.P. Tan, T. Blon, B. Chaudret and M. Respaud, *Appl. Phys. Lett.* **95**, 152504 (2009).
  - [10] T. Maurer, F. Ott, G. Chaboussant, Y. Soumare, J.-Y. Piquemal and G. Viau, *Appl. Phys. Lett.* **91**, 172501 (2007).
  - [11] A. Encinas-Oropesa, M. Demand, L. Piraux, I. Huynen and U. Ebels, *Phys. Rev. B* **63**, 104415 (2001).
  - [12] F. Zighem, T. Maurer, F. Ott and G. Chaboussant, *Journal of Applied Physics*, **109**, 013910 (2011).
  - [13] K. Nielsch, R. B. Wehrspohn, J. Barthel, J. Kirschner, U. Gosele, S. F. Fischer and H. Kronmüller., *Appl. Phys. Lett.* **79**, 1360-1362 (2001).
  - [14] A. N. Dobrynin, V. M. T. S. Barthem and D. Givord, *Appl. Phys. Lett.* **95**, 052511 (2009) .
  - [15] O. Henkel, *Phys. Status Solidi* **7**, 919-929 (1964).
  - [16] J. Garcia-Otero, M. Porto and J. Rivas, *J. Appl. Phys.*, **87**, 7376-7381 (2000).
  - [17] F. Ott, T. Maurer, G. Chaboussant, Y. Soumare, J.-Y. Piquemal and G. Viau, *J. Appl. Phys.* **105**, 013915 (2009).
  - [18] T. Maurer, F. Zighem, F. Ott, G. Chaboussant, G. André, Y. Soumare, J.Y. Piquemal, G. Viau and C. Gatel, *Phys. Rev. B* **80**, 064427 (2009).
  - [19] D. C. Meeker, *Finite Element Method Magnetics*. The FEMM package is freely available at <http://www.femm.info>.

- [20] P. E. Tannenwald and R. Weber, Phys. Rev. **121**, 715 (1961).
- [21] T. Fischbacher, M. Franchin, G. Bordinon and H. Fangohr, IEEE Trans. Mag. **43**, 2896 (2007), URL : <http://nmag.soton.ac.uk/nmag/>
- [22] NETGEN, URL: <http://www.hpfem.jku.at/netgen/>
- [23] E.P. Wohlfarth, J. Appl. Phys. **29**, 595 (1958).